

Quantum Chemical Investigation of Formation of Polychlorodibenzo-*p*-Dioxins and Dibenzofurans from Oxidation and Pyrolysis of 2-Chlorophenol

Mohammednoor Altarawneh, Bogdan Z. Dlugogorski,* Eric M. Kennedy, and John C. Mackie*

Process Safety and Environment Protection Research Group, School of Engineering, The University of Newcastle, Callaghan, New South Wales 2308, Australia

Received: August 28, 2006; In Final Form: January 21, 2007

Density functional theory (DFT) calculations have been used to obtain thermochemical parameters for formation of polychlorinated dibenzo-*p*-dioxins and dibenzofurans (PCDD/PCDF) from the oxidation of 2-chlorophenol. Formation mechanisms of PCDD through radical–radical coupling have been investigated in detail. The sequence of 2-chlorophenoxy radical coupling has been studied. The formation of chlorinated bis keto dimers which results from cross coupling of 2-chlorophenoxy at the *ortho* carbon bearing hydrogen (a known direct route for PCDF formation) passes through a tight transition structure whose barrier is 9.4 kcal/mol (0 K). Three routes for the formation of the most abundant PCDD/PCDF species (viz., 4,6-dichlorodibenzofuran, 4,6-DCDF, and 1-monochlorodibenzo-*p*-dioxin, 1-MCDD) in oxidation and pyrolysis of 2-chlorophenol are discussed. In the case of 4,6-DCDF, formation through H or $\text{HO} + \text{keto-keto} \rightleftharpoons \text{H}_2$ or $\text{H}_2\text{O} + \text{keto-keto} \rightleftharpoons \text{H}_2$ or $\text{H}_2\text{O} + \text{enol-keto} \rightleftharpoons \text{H}_2$ or $\text{H}_2\text{O} + 4,6\text{-DCDF} + \text{HO}$ is shown to be the preferred route. The other two routes proceed via closed shell processes ($\text{keto-keto} \rightleftharpoons \text{enol-keto} \rightleftharpoons \text{enol-enol} \rightleftharpoons \text{H}_2\text{O} + 4,6\text{-DCDF}$) and ($\text{keto-keto} \rightleftharpoons \text{enol-keto} \rightleftharpoons (\text{H}\cdot, \text{OH}\cdot) 4,6\text{-DCDF} \rightleftharpoons \text{H}_2\text{O} + 4,6\text{-DCDF}$). Results indicate that 1-MCDD should be the favored product in 2-chlorophenol pyrolysis in agreement with experimental findings. According to our results, tautomerization (inter-ring hydrogen transfer) and intra-annular displacement of HCl would not be competitive with paths deriving from H abstraction from the phenolic oxygen and the benzene ring followed by displacement of Cl in the formation of dibenzo-*p*-dioxin (DD) and 1-MCDD. The results presented here will assist in construction of detailed kinetic models to account for the formation of PCDD/PCDF from chlorophenols.

Introduction

Owing to their extreme toxicity in the environment, dibenzo-*p*-dioxins and furans (PCDD/PCDF) have been the focus of much scientific, social, and technical attention. They are formed both by surface mediated processes and through gaseous reactions of precursors, especially chlorophenols. Phenoxy radical–radical recombinations, radical–molecule couplings of phenoxy and phenol, and reactions involving phenol molecules comprise most of the proposed pathways to account for PCDD/PCDF formation in the gas phase.^{1–6} An understanding of the detailed mechanisms which govern these chemical processes is of great significance in building reliable kinetic models that could account for the contribution of the gaseous route in the production of PCDD/PCDF in combustion processes.

The importance of the gas-phase route to the formation of PCDD/PCDF has been reconsidered^{7–9} owing to the previous underestimation of the yields of PCDD/PCDF in the gas phase. Underestimation resulted from the assumption of rapid consumption of phenoxy radical by molecular oxygen.^{10,11} In earlier kinetic models for formation of PCDD/PCDF in the gas phase, it was assumed that only PCDD (and not PCDF) could be formed from chlorinated phenols through radical–molecule

reactions.^{12–14} It was assumed that self-reactions of phenoxy radicals were too slow to compete with their oxidation and decomposition. Thus, self-recombination of the phenoxy radicals was not included in the original kinetics models. However, recent work has shown that the dimerization of chlorinated phenoxy radicals is the major pathway in the formation of PCDD as well as PCDF.^{5,15–17}

The potential of the chlorinated phenoxy radicals to form PCDD/PCDF has been investigated experimentally in slow combustion systems where the reaction time is between 2 and 100 s.^{17–22} Dimerization of the phenol and phenoxy radicals has also been studied^{23,25–27} quantum chemically to determine possible products and to elucidate mechanisms of formation of PCDD/PCDF. Through the combination of two phenoxy radicals, six different dimers have been located,²³ including *o,o'*-dihydroxybiphenyl (DOBP) and *o*-phenoxyphenol (POP). The formation of PCDF is often attributed to the formation of DOBP which results from radical–radical combination, while the formation of PCDD is attributed to the formation of POP²¹ which could result from either radical–radical or radical–molecule reactions.

The branching ratio between PCDD and PCDF depends primarily on the position of the chlorine on the phenyl ring where only two chlorophenoxy radicals with at least one *ortho* hydrogen atom are capable of forming PCDF and two chlo-

* To whom correspondence should be addressed. Tel: (+61 2) 4921 6176. Fax: (+61 2) 4921 6920. E-mail: Bogdan.Dlugogorski@newcastle.edu.au.

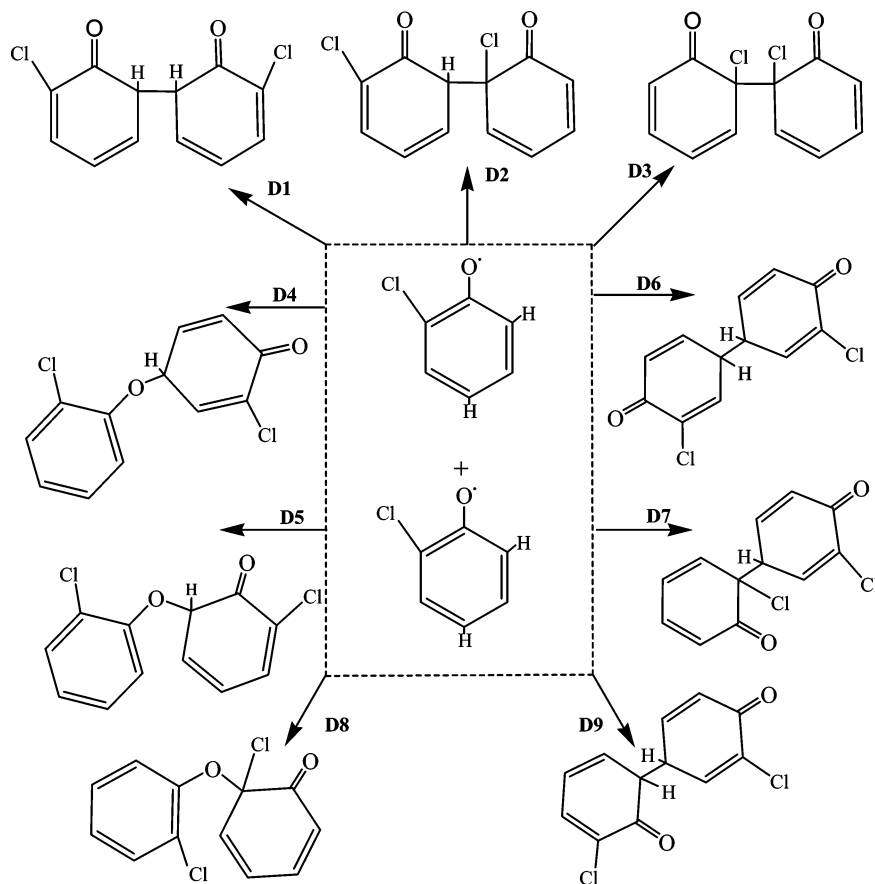


Figure 1. Stable structures from the dimerization of two 2-chlorophenoxy radicals.

rophenoxy radicals with chlorine in the *ortho* position could form PCDD.²¹ However, the presence of active radicals¹⁹ in the combustion environment and interconversion channels²³ between the two phenoxy radical dimers can have a significant impact on the distribution of the PCDD/PCDF isomers.

In the present work, we have carried out density functional theory (DFT) calculations on the oxidation of 2-chlorophenol leading to the formation of the main observed products in its slow oxidation^{17,19} and pyrolysis.¹⁸ These products are principally DD, 1-MCDD, 4,6-DCDF, and 4-MCDF (4-monochlorodibenzofuran). The role of radicals H, OH, and Cl in propagating reactions has been extensively investigated.

Computational Details

All calculations were performed with the Gaussian 03 suite of programs.²⁸ Optimized geometries and harmonic vibrational frequencies of all species and transition structures on the reaction potential energy surface have been calculated using the hybrid DFT of B3LYP which employs the three parameter Becke exchange functional, B3,²⁹ with the Lee–Yang–Parr nonlocal correctional functional LYP³⁰ along with the polarized basis set of 6-31G(d).³¹ As we are concerned with relatively large molecular species, high accuracy methods such as G3 are not appropriate, thus single point energy calculations with the extended basis set of 6-311+G(3df, 2p) have been performed on the geometry obtained with the 6-31G(d) basis set to obtain reliable energies. Following the conventional notation in computational chemistry, this approach is denoted as B3LYP/6-311+G(3df,2p)//B3LYP/6-31G(d)+ZPVE(B3LYP/6-31G(d)). Zhu and Bozzelli³² have shown that this approach yields reliable energies for PCDD/PCDF. Stationary points on reaction

potential energy surfaces (PESs) were characterized either as minima or transition structures (TSs) through the analysis of their vibrational frequencies where transition structures contain one and only one imaginary frequency along the reaction coordinate. The unrestricted UB3LYP has been used to optimize the open shell singlet structures such as the biradical transition structures of 2-chlorophenoxy self-condensation shown in Figure 1. Where convergence of the unrestricted procedure to an expectation value of $S^2 = 0$ resulted, stability testing of the wavefunction was made with reoptimization, where necessary. Where appropriate, IRC calculations have been used to link the reactant and product with their transition structures. Geometries obtained at B3LYP/6-31G(d) along with single point energy values at the larger basis set have been used to calculate the energetic parameters required to derive the free energy profiles for all reactions considered at 298, 400, 500, 600, 700, 800, 900, and 1000 K using statistical thermodynamics formulas.

Optimized geometries (Cartesian coordinates), rotational constants, vibration frequencies, total energies, and zero point energies of all equilibrium and transition structures are given in the Supporting Information.

Results and Discussion

The various reaction pathways leading to the formation of PCDD/PCDF from the different possible combinations of 2-chlorophenol and 2-chlorophenoxy are presented herein. Reaction schemes embedded with energies and energy barriers at 0 K are displayed in Figures 1–7. Tables 1–5 provide values of both the Gibbs free energy change of reaction and activation, for the temperature of interest (298.15–1000 K). Although the

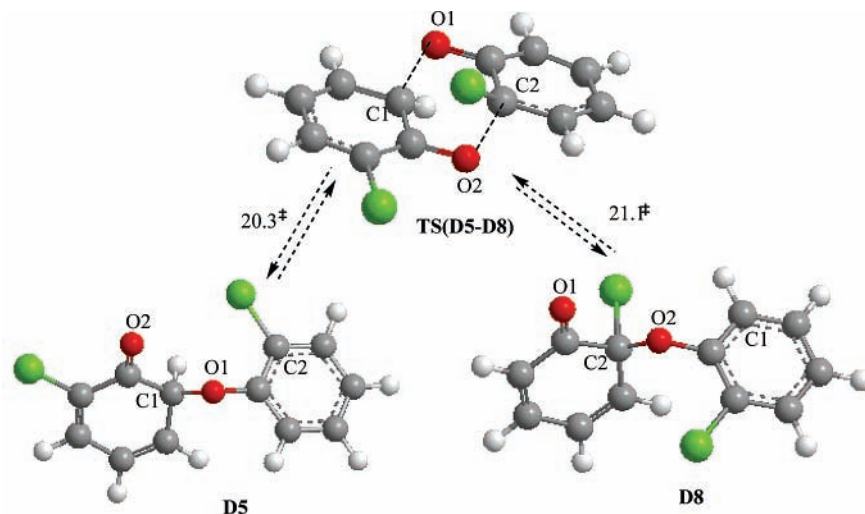


Figure 2. ‘Stair type’ transition structure for the interconversion process between 2-chloro-6-(2-chlorophenoxy)cyclohexa-2,4-dienone and 6-chloro-6-(2-chlorophenoxy)cyclohexa-2,4-dienone. Symbol † denotes activation energies at 0 K computed at the B3LYP/6-311+G(3df,2p)//B3LYP/6-31G(d) level of theory.

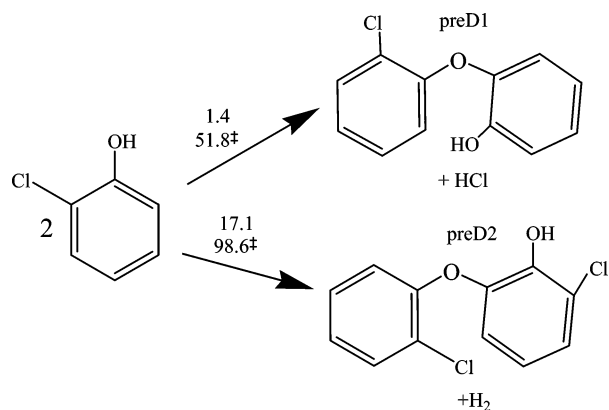


Figure 3. Self-condensation of 2-chlorophenol. With respect to the numbers above the arrows, upper values denote the reaction energies and the lower (†) signify the activation energies (kcal/mol) at 0 K.

discussion in the text is mainly based on E values at 0 K, $\Delta_r G^0$ and ΔG^\ddagger at 298–1000 K, when significantly different from their corresponding values of $\Delta_r E^0$ and E_a , are also introduced to call attention to the entropy contribution.

Self-Condensation of 2-Chlorophenoxy Radical. The unpaired electron in the 2-chlorophenoxy radical is delocalized, and radical character appears at the phenolic oxygen, the *para* carbon, and the *ortho* carbon bonded to hydrogen as well as the *ortho* carbon bonded to chlorine (Figure 8). Electron density calculations²⁵ revealed that 41.3 and 39.1% of the unpaired spin density are located on the phenyl oxygen (O/) and the *para*-carbon (*p*-CH/), respectively, in the keto resonance structure (mesomer) of the phenoxy radical. Taking into account the significant stability of the phenoxy and chlorophenoxy radicals,³³ because of their resonance stabilization energy, in a combustion or pyrolysis environment, chlorophenoxy radicals could build up in appreciable concentrations to enable self-condensation to occur.

There are ten possible mesomers that could result from the self-condensation of 2-chlorophenoxy radical. The peroxide structure involving O//O coupling could not be optimized to a stationary point at the B3LYP/6-31G(d) level of theory, thus, in total, 9 stable structures have been determined for the self-combination of 2-chlorophenoxy radicals (Figure 1).

The possible coupling products of two 2-chlorophenoxy radicals are

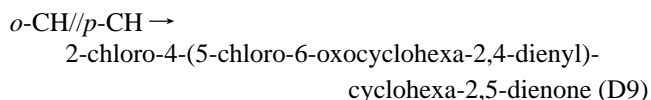
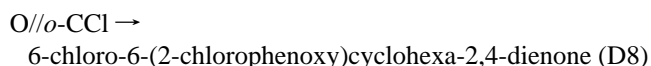
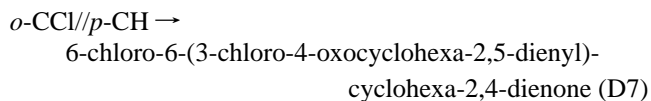
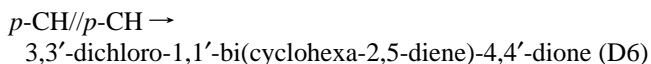
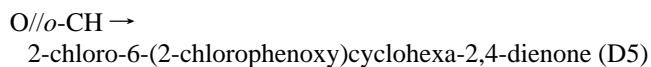
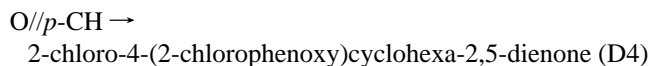
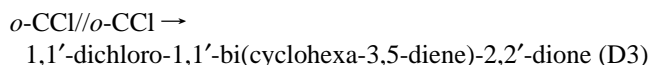
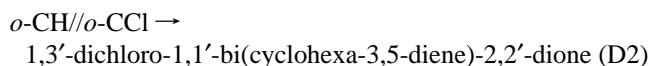
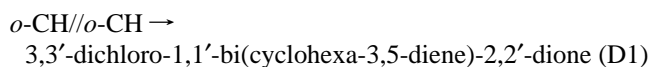


Table 6 summarizes the activation energies and energy changes of the reactions as derived from the results computed at 0 K at the B3LYP/6-311+G(3df,2p)//B3LYP/6-31G(d) level of theory. Table 1 further characterizes the formation of D1–D9 in terms of $\Delta_r G^0$ and ΔG^\ddagger , between 298 and 1000 K. Large entropic penalty associated with the loss of a molecule during formation of all coupling products (D1–D9) increases both free energy of activation and free energy change of all reactions. However, Table 1 does not modify the thermodynamic and kinetic ordering of the coupling products, enunciated in Table 6. The inspection of free energies of activation of Table 1 yields the following kinetic ordering of the coupling products through-

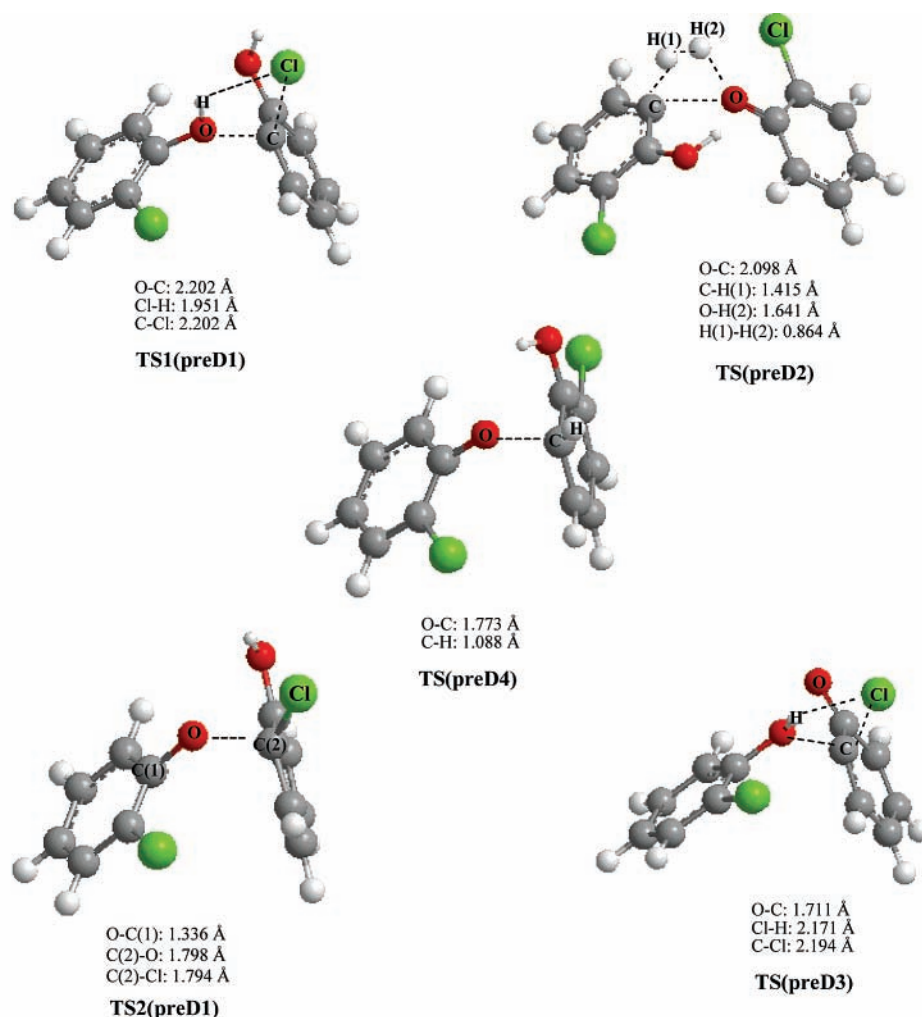


Figure 4. Transition structures for self-condensation of 2-chlorophenol and combination of 2-chlorophenol with 2-chlorophenoxy.

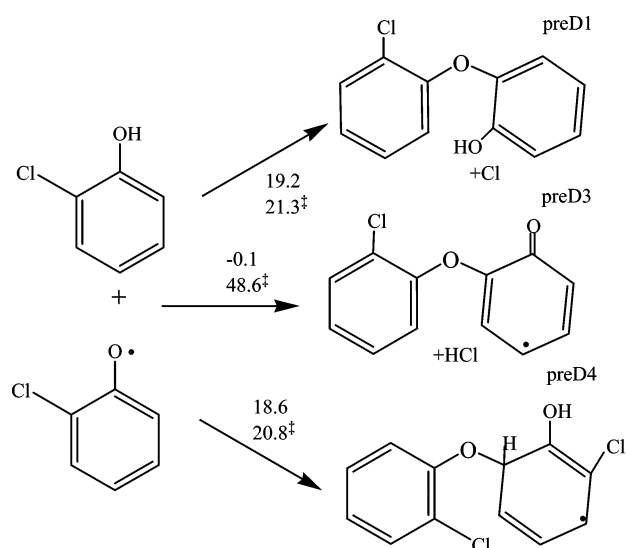


Figure 5. Pathways to predioxins from the combination of 2-chlorophenol and 2-chlorophenoxy. Upper values are the reaction energies and lower values (‡) are the activation energies in kcal/mol at 0 K.

out most of the temperature regime $D3 > D7 > D2 > D5 > D4 > D9 > D1$.

The combinations of the oxygen-centered radical mesomer (O) with the *ortho* carbon-hydrogen centered radical mesomer (*o*-CH) and the oxygen-centered radical mesomer with the *ortho*

carbon-chlorine centered radical mesomer (*o*-CCl) produce the keto-ether structures of D5 and D8, respectively. These can be regarded as predioxin structures. The formation of D8 is slightly more exoergic than D5 formation (by 1.5 kcal/mol at 0 K). Formation of D5 requires activation energy of 9.0 kcal/mol at 0 K, while the formation of D8 appears to be barrierless, possibly because of the large fraction of the unpaired electron density located on the phenolic oxygen. Additionally, no transition structure could be found for the cross coupling of two 2-chlorophenoxy radicals at the *para* carbon to afford D6 where again the large electron density at this position would seem to enable the coupling to occur without a barrier based on E_a values in Table 6. Although the formation of D5, D6, and D8 is quite exoergic in terms of $\Delta_r E^0$, by contrast the $\Delta_r G^0$ estimate, between 298 and 1000 K, indicates increasing endoergic with temperature.

The most exoergic reaction at 0 K produces D4 and results from cross coupling of the phenolic oxygen with the *para* carbon. A transition structure with a trivial barrier of 1.2 kcal/mol (0 K) was found for the coupling of two 2-chlorophenoxy to produce D4. This trivial barrier constitutes an artifact, since its appearance is related to the size of a basis set deployed in computation. We expect the barrier to vanish, if a bigger basis set were employed in the optimization. Based on transition structure, its ΔG^\ddagger is calculated to 19.4 kcal/mol at 298 K, increasing dramatically with temperature to reach 54.5 kcal/mol at 1000 K. Formation of D4 constitutes the most direct

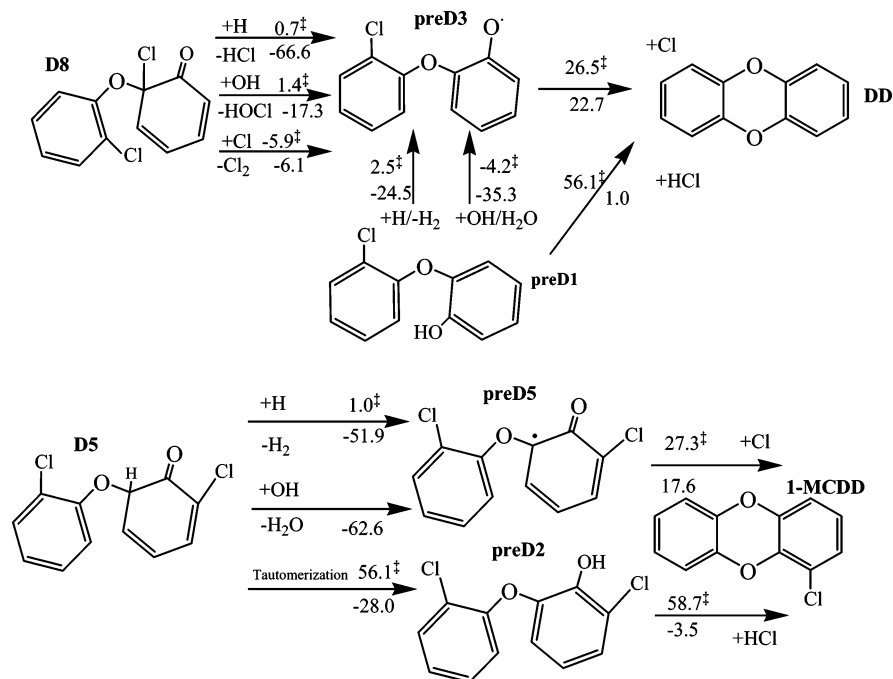


Figure 6. Radical–molecule and radical–radical pathways for the formation of dibenzodioxin (DD) and 1-monochlorodibenzo-*p*-dioxin (1-MCDD). Symbol [‡] denotes activation energies, and the other values are the reaction energies both calculated at the B3LYP/6-311+G(3df,2p)//B3LYP/6-31G(d) level of theory at 0 K.

route to 4-phenoxyphenol, which was found to be the main experimental product for phenoxy self-combination in a smog chamber.¹⁵

The most likely route to 4-phenoxyphenol is through H-transfer of the hydrogen at the 4-position of the D4 moiety to the phenolic oxygen through intramolecular transfer. However, the computed activation energy barrier for this process is extremely high (95 kcal/mol at 0 K). Thus intermolecular H transfer is expected to be the dominant pathway. D4 is not a direct precursor for the formation of PCDD or PCDF but has been found to be an intermediate in the formation of the polychlorophenoxy ethers.¹⁵

In addition to formation of D4, certain coupling modes of 2-chlorophenoxy radicals produce dimerization products that do not lead to the formation of PCDD or PCDF. Coupling of both CH/ and CCl/ centered radical mesomers at the *para* carbon produces D7 and D9. Formation of D9 is preferred over the formation of D7 both thermodynamically and kinetically. D1, D2, and D3, in addition to providing channels for formation of PCDF (next paragraph), could be regarded as precursors to the formation of chlorinated naphthalene^{18–19,36} (which has been found in the oxidation and pyrolysis of 2-chlorophenol) through elimination of CO. However, examination of these routes is outside the scope of the present work.

Formation of PCDF is generally considered to arise from the coupling of two chlorophenoxy radicals at the hydrogen substituted carbons at the *ortho* positions.²¹ Due to the spin density distribution within the 2-chlorophenoxy system with most of the density located on the phenolic oxygen and the *para* carbon, cross coupling between 2-chlorophenoxy at the *ortho* hydrogen to produce the most direct routes to PCDF (the chlorinated *o,o'*-dihydroxybiphenyl) passes through tight transition structures. For *ortho*-substituted chlorine, the lowest barrier for *ortho*–*ortho* coupling occurs for *o*-CH//*o*-CH coupling (D1, 9.4 kcal/mol at 0 K with ΔG^\ddagger increasing to 22.0, 30.3, and 50.4 kcal/mol at 298, 500, and 1000 K, respectively). The barrier is highest for *o*-CCl//*o*-CCl coupling (D3, 19.1 kcal/mol at 0 K, with ΔG^\ddagger increasing to 32.4, 41.3, and 62.9 kcal/mol at 298,

500, and 1000 K respectively). Hence, based on computed reaction energies and activation barriers at elevated temperatures, we would expect the yields of *ortho*–*ortho* coupling products to follow D1 > D2 > D3.

Interconversion of 2-Chlorophenoxy Dimers. Interconversion may occur between the dimerized structures resulting from the coupling of 2-chlorophenoxy. Such processes are analogous to the interconversion between (nonchlorinated) phenoxy coupling dimers.^{16,23,26} These interconversions can modify the initial distribution of dimers and the final concentration of the PCDD/PCDF congeners. Although we found transition structures for these interconversion processes at the HF/3-21G level of theory, we have been unsuccessful in locating the interconversion channel between the most likely abundant dimer (D4) and the PCDD prestructures D5 and D8 or the PCDF prestructures D1 and D2 at the B3LYP/6-31G(d) level of theory. However, we have discovered a parallel ring ‘stair type’ transition structure for the rearrangement of D5 into D8 as shown in Figure 2. This transition structure represents concentric movements between the phenolic oxygen atoms in D5 and D8 and the carbon bearing *ortho* H in D5 and the carbon bearing chlorine atom in D8. Atom labels in Figure 2 show the structural arrangements on each side of this transition structure.

As will be shown in the next section, D5 is a prestructure for 1-monochlorodibenzo-*p*-dioxin (1-MCDD), and D8 is the prestructure for the nonchlorinated dibenzo-*p*-dioxin (DD). The computed difference in values of ΔG^\ddagger within the temperature range of 298–1000 K, for the conversion of D5 to D8 and vice versa through this parallel ring transition structure, is negligible (<1 kcal/mol). Hence, the interconversion of D5 and D8, via this transition structure, should not significantly alter the distribution between the two most abundant PCDD species in the oxidation of 2-chlorophenol.

Formation of Polychlorinated Dibenzo-*p*-Dioxins. Notionally, PCDD could result from direct intermolecular condensation through reaction of molecule + molecule (2-chlorophenol + 2-chlorophenol), molecule + radical (2-chlorophenol + 2-chlorophenoxy), and radical + radical (2-chlorophenoxy + 2-chlo-

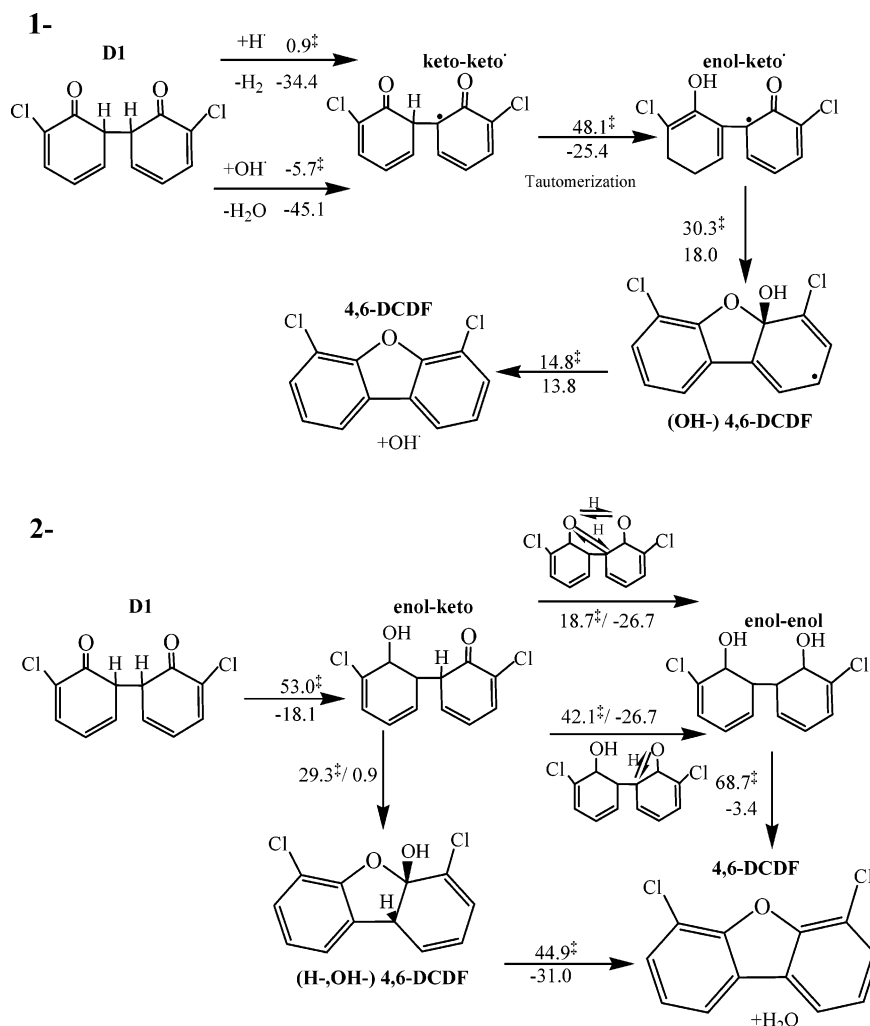


Figure 7. Formation of 4,6-DCDF from 3,3'-dichloro-1,1'-bi(cyclohexa-3,5-diene)-2,2-dione (D1). Symbol [‡] denotes activation energies, and the other values are the reaction energies at 0 K, both calculated at the B3LYP/6-311+G(3df,2p)//B3LYP/6-31G(d) level of theory.

TABLE 1: Values of $\Delta_r G^\circ$ and ΔG^\ddagger (kcal/mol), at Temperatures Relevant to PCDD/PCDF Formation in the Gas Phase, for the Coupling Reactions of Two 2-Chlorophenoxy Radicals To Produce D1–D9

| no. | T (K) | | 298.15 | 400 | 500 | 600 | 700 | 800 | 900 | 1000 |
|-----|-------------------------------------|---------------------|--------|------|------|------|------|------|------|------|
| 1 | 2(2-chlorophenoxy) \rightarrow D1 | $\Delta_r G^\circ$ | 4.1 | 8.3 | 12.4 | 16.4 | 20.4 | 24.4 | 28.3 | 32.2 |
| | | ΔG^\ddagger | 22.1 | 26.2 | 30.3 | 34.3 | 38.4 | 42.4 | 46.4 | 50.4 |
| 2 | 2(2-chlorophenoxy) \rightarrow D2 | $\Delta_r G^\circ$ | 13.8 | 18.3 | 22.6 | 26.9 | 31.2 | 35.4 | 39.7 | 43.9 |
| | | ΔG^\ddagger | 28.6 | 33.2 | 37.4 | 41.7 | 45.9 | 50.2 | 54.4 | 58.6 |
| 3 | 2(2-chlorophenoxy) \rightarrow D3 | $\Delta_r G^\circ$ | 21.6 | 25.9 | 30.1 | 34.2 | 38.2 | 42.2 | 46.2 | 50.1 |
| | | ΔG^\ddagger | 32.4 | 36.9 | 41.3 | 45.7 | 50.8 | 54.3 | 58.6 | 62.9 |
| 4 | 2(2-chlorophenoxy) \rightarrow D4 | $\Delta_r G^\circ$ | -5.1 | -1.5 | 3.7 | 7.7 | 11.6 | 14.9 | 18.7 | 22.6 |
| | | ΔG^\ddagger | 19.4 | 24.5 | 29.4 | 34.4 | 39.4 | 44.5 | 49.5 | 54.5 |
| 5 | 2(2-chlorophenoxy) \rightarrow D5 | $\Delta_r G^\circ$ | -1.2 | 2.8 | 6.7 | 10.6 | 14.4 | 18.2 | 21.9 | 25.6 |
| | | ΔG^\ddagger | 19.7 | 25.3 | 28.1 | 36.8 | 40.5 | 42.4 | 48.2 | 53.7 |
| 6 | 2(2-chlorophenoxy) \rightarrow D6 | $\Delta_r G^\circ$ | 5.8 | 9.8 | 13.6 | 17.5 | 21.2 | 25.3 | 28.7 | 32.3 |
| | | ΔG^\ddagger | 9.2 | 13.2 | 17.3 | 21.3 | 25.3 | 29.3 | 33.2 | 37.1 |
| 7 | 2(2-chlorophenoxy) \rightarrow D7 | $\Delta_r G^\circ$ | 30.4 | 35.1 | 39.7 | 44.3 | 48.9 | 53.5 | 58.1 | 62.7 |
| | | ΔG^\ddagger | -2.1 | 2.1 | 6.1 | 10.1 | 14.1 | 18.7 | 21.9 | 25.7 |
| 8 | 2(2-chlorophenoxy) \rightarrow D8 | $\Delta_r G^\circ$ | 5.8 | 9.9 | 13.9 | 17.8 | 21.7 | 25.6 | 29.4 | 33.2 |
| | | ΔG^\ddagger | 21.9 | 26.3 | 30.6 | 34.9 | 39.2 | 43.4 | 47.6 | 51.8 |

phenoxy). Breaking of the O–H bond of the hydroxyl group in 2-chlorophenol to produce 2-chlorophenoxy radical is a highly endothermic process, thus paths through molecule + molecule have lower reaction energies compared with paths through molecule + radical or radical + radical unless the O–H bond is broken by heterogeneous or wall effects, ultraviolet light, or through H abstraction by radicals such as H or OH. Twelve pathways for PCDD formation from 2,4,5-trichlorophenol (TCP) have been investigated previously,²⁷ and the distributions of

PCDD congeners are found to be dependent on the formation pathways (molecule, radical) and on the ring closure mechanism involved. Our calculated results are similar to those quoted²⁷ for self-condensation of TCP.

Figure 3 illustrates pathways for the self-condensation of 2-chlorophenol into the predioxin structures 2-(2-chlorophenoxy)phenol (preD1) and 2-chloro-6-(2-chlorophenoxy)phenol (preD2). The figure also includes reaction energies and energy barriers at 0 K. Elimination of HCl upon attack of the hydroxyl

TABLE 2: Values of $\Delta_r G^\circ$ and ΔG^\ddagger (kcal/mol), at Temperatures Relevant to PCDD/PCDF Formation in the Gas Phase, for the Coupling Reactions of Two 2-Chlorophenol Molecules To Form the Predioxin Structures PreD1 and PreD2^a

| no. | T (K) | | 298.15 | 400 | 500 | 600 | 700 | 800 | 900 | 1000 |
|-----|--|---------------------|--------|------|------|-------|-------|-------|-------|-------|
| 10 | 2(2-chlorophenol) \rightarrow PreD1 + HCl | $\Delta_r G^\circ$ | 4.2 | 4.7 | 5.1 | 5.5 | 5.9 | 6.2 | 6.6 | 6.9 |
| | | ΔG^\ddagger | 63.5 | 67.4 | 71.2 | 75.6 | 78.7 | 82.4 | 86.1 | 89.7 |
| 11 | 2(2-chlorophenol) \rightarrow PreD2 + H ₂ | $\Delta_r G^\circ$ | 23.4 | 25 | 26.5 | 27.9 | 29.3 | 30.7 | 32.5 | 33.4 |
| | | ΔG^\ddagger | 110.6 | 115 | 118 | 121.8 | 125.4 | 128.9 | 132.8 | 136.6 |
| 12 | 2-chlorophenol + 2-chlorophenoxy \rightarrow PreD1 + Cl | $\Delta_r G^\circ$ | -0.5 | 0.7 | 1.9 | 3.0 | 3.0 | 4.1 | 5.0 | 6.1 |
| | | ΔG^\ddagger | 33.3 | 37.3 | 41.3 | 45.2 | 49.1 | 52.9 | 56.7 | 60.5 |
| 13 | 2-chlorophenol + 2-chlorophenoxy \rightarrow PreD3 + HCl | $\Delta_r G^\circ$ | 1.8 | 2.1 | 2.4 | 2.6 | 2.8 | 2.9 | 3.1 | 3.2 |
| | | ΔG^\ddagger | 62.1 | 66 | 69.7 | 73.5 | 77.2 | 80.8 | 84.5 | 88.1 |
| 14 | 2-chlorophenol + 2-chlorophenoxy \rightarrow PreD4 | $\Delta_r G^\circ$ | 30.5 | 34.6 | 38.5 | 42.4 | 46.2 | 50 | 53.7 | 57.4 |
| | | ΔG^\ddagger | 32.7 | 36.7 | 40.7 | 44.6 | 48.5 | 52.4 | 56.2 | 60.1 |

^a Rows 12–14 provide $\Delta_r G^\circ$ and ΔG^\ddagger for the reactions of 2-chlorophenol with 2-chlorophenoxy, which produce predioxin structures PreD1, PreD3, and PreD4.

TABLE 3: Values of $\Delta_r G^\circ$ and ΔG^\ddagger (kcal/mol) for the Formation of DD and 1-MCDD from D8 and D5^a

| no. | T (K) | | 298.15 | 400 | 500 | 600 | 700 | 800 | 900 | 1000 |
|-----|---|---------------------|--------|-------|-------|-------|-------|-------|-------|-------|
| 16 | D8 + H \rightarrow preD3 + HCl | $\Delta_r G^\circ$ | -72.4 | -74 | -75 | -76 | -76.9 | -77.8 | -78.7 | -80.0 |
| | | ΔG^\ddagger | 4.8 | 6.3 | 7.8 | 9.4 | 11.0 | 12.6 | 14.2 | 15.8 |
| 17 | D8 + OH \rightarrow preD3 + HOCl | $\Delta_r G^\circ$ | -20.6 | -21.5 | -22.3 | -23.0 | -23.5 | -24.1 | -24.6 | -25.0 |
| | | ΔG^\ddagger | 9.0 | 11.5 | 14.1 | 16.7 | 19.2 | 21.8 | 24.8 | 26.9 |
| 18 | D8 + Cl \rightarrow preD3 + Cl ₂ | $\Delta_r G^\circ$ | -9.5 | -14.7 | -20.0 | -25.1 | -30.4 | -35.7 | -41.0 | -46.3 |
| | | ΔG^\ddagger | 17.0 | 14.9 | 12.7 | 10.4 | 8.1 | 5.7 | 3.2 | 0.7 |
| 19 | preD1 + H \rightarrow H ₂ + preD3 | $\Delta_r G^\circ$ | -24.5 | -25 | -25 | -25.3 | -25.5 | -25.7 | -25.8 | -26.0 |
| | | ΔG^\ddagger | 8.8 | 11.2 | 13.7 | 16.2 | 18.7 | 21.3 | 23.8 | 26.3 |
| 20 | preD1 + OH \rightarrow H ₂ O + preD3 | $\Delta_r G^\circ$ | -37.5 | -38 | -38 | -37.4 | -37.3 | -37.1 | -36.8 | -37.0 |
| | | ΔG^\ddagger | 4.1 | 4.9 | 8.3 | 10.5 | 14.7 | 18.5 | 20.5 | 23.1 |
| 21 | preD3 \rightarrow DD + Cl | $\Delta_r G^\circ$ | 9.3 | 7.1 | 5.0 | 2.7 | 0.5 | -1.7 | -3.9 | -6.1 |
| | | ΔG^\ddagger | 29.0 | 30.1 | 31.2 | 32.3 | 33.4 | 34.6 | 35.8 | 37.0 |
| 22 | preD1 \rightarrow DD + HCl | $\Delta_r G^\circ$ | -13.6 | -17.0 | -19.4 | -21.9 | -25.0 | -27.0 | -29.8 | -32.0 |
| | | ΔG^\ddagger | 57.5 | 58.1 | 58.8 | 59.6 | 60.4 | 61.2 | 62.0 | 62.8 |
| 23 | D5 + H \rightarrow H ₂ + preD5 | $\Delta_r G^\circ$ | -50.4 | -51 | -51 | -51.4 | -51.7 | -52.1 | -52.4 | -53.3 |
| | | ΔG^\ddagger | 6.9 | 9.2 | 11.5 | 13.7 | 16.2 | 18.3 | 20.7 | 23.0 |
| 24 | D5 + OH \rightarrow H ₂ O + preD5 | $\Delta_r G^\circ$ | -63.4 | -63.4 | -63.4 | -63.5 | -63.5 | -63.5 | -63.4 | -63.1 |
| | | ΔG^\ddagger | 57.0 | 57.3 | 57.7 | 58.1 | 58.3 | 58.6 | 59.0 | 59.3 |
| 25 | D5 \rightarrow preD2 | $\Delta_r G^\circ$ | -26.3 | -25.0 | -24.7 | -23.7 | -23.0 | -22.7 | -20.9 | -20.2 |
| | | ΔG^\ddagger | 58.7 | 58.7 | 58.7 | 58.6 | 58.6 | 58.5 | 58.5 | 58.4 |
| 26 | preD2 \rightarrow HCl + 1-MCDD | $\Delta_r G^\circ$ | -12.8 | -16 | -20.0 | -23.3 | -27.0 | -30.0 | -33.8 | -37.5 |
| | | ΔG^\ddagger | 58.7 | 58.7 | 58.7 | 58.6 | 58.6 | 58.5 | 58.5 | 58.4 |
| 27 | preD5 \rightarrow Cl + 1-MCDD | $\Delta_r G^\circ$ | 11.2 | 9.2 | 7.2 | 5.2 | 3.2 | 1.3 | -0.7 | -2.5 |
| | | ΔG^\ddagger | 29.7 | 30.7 | 31.7 | 32.8 | 33.9 | 35.0 | 36.1 | 37.2 |

^a In reference to Figure 6.

TABLE 4: Values of $\Delta_r G^\circ$ and ΔG^\ddagger (kcal/mol) for Reactions Involving the Formation of 4,6-DCDF from D1^a

| no. | T (K) | | 298.15 | 400 | 500 | 600 | 700 | 800 | 900 | 1000 |
|-----|---|---------------------|--------|-------|-------|-------|-------|-------|-------|-------|
| 28 | D1+H \rightarrow H ₂ + keto-keto' | $\Delta_r G^\circ$ | -43.9 | -44.4 | -45 | -45.5 | -46.1 | -46.6 | -47.1 | -47.6 |
| | | ΔG^\ddagger | 7.0 | 9.3 | 11.7 | 14.1 | 16.5 | 18.9 | 21.3 | 23.8 |
| 29 | D1 + OH \rightarrow keto-keto' + H ₂ O | $\Delta_r G^\circ$ | -56.2 | -56.9 | -57.5 | -58.2 | -58.8 | -59.4 | -60.0 | -60.6 |
| | | ΔG^\ddagger | 2.7 | 6.0 | 9.2 | 12.5 | 15.7 | 18.9 | 22.1 | 25.3 |
| 30 | keto-keto' \rightarrow enol- keto' | $\Delta_r G^\circ$ | -24.2 | -23.7 | -23.2 | -22.6 | -22 | -21.5 | -20.9 | -20.3 |
| | | ΔG^\ddagger | 49.0 | 49.4 | 49.7 | 50.0 | 50.4 | 50.7 | 51.1 | 51.5 |
| 31 | enol-keto' \rightarrow (OH-) 4,6-DCDF | $\Delta_r G^\circ$ | 18.1 | 18.3 | 18.5 | 18.6 | 18.8 | 18.9 | 19.0 | 19.1 |
| | | ΔG^\ddagger | 35.2 | 35.6 | 36.2 | 36.8 | 37.4 | 38.1 | 38.8 | 39.6 |
| 32 | (OH-) 4,6-DCDF \rightarrow OH + 4,6-DCDF | $\Delta_r G^\circ$ | 5.2 | 2.0 | -1.1 | -4.3 | -7.3 | -10.4 | -13.4 | -16.4 |
| | | ΔG^\ddagger | 14.6 | 14.4 | 14.3 | 14.2 | 14.2 | 14.1 | 14.1 | 14.1 |
| 33 | D1 \rightarrow enol-keto | $\Delta_r G^\circ$ | -17.5 | -17.3 | -17.1 | -16.9 | -16.8 | -16.6 | -16.4 | -16.2 |
| | | ΔG^\ddagger | 53.2 | 53.3 | 53.4 | 53.5 | 53.5 | 53.6 | 53.8 | 53.9 |
| 34 | enol-keto \rightarrow (OH-,H-) 4,6-DCDF | $\Delta_r G^\circ$ | 18.1 | 18.4 | 19.2 | 19.3 | 19.3 | 19.5 | 19.6 | 19.8 |
| | | ΔG^\ddagger | 30.4 | 31.0 | 31.5 | 32.1 | 32.7 | 33.4 | 34.0 | 34.7 |
| 35 | enol-keto \rightarrow enol-enol concentric TS(enol-keto \rightarrow enol-enol) | $\Delta_r G^\circ$ | -26 | -25.7 | -25.4 | -25.1 | -24.8 | -24.6 | -24.3 | -24 |
| | | ΔG^\ddagger | 20.0 | 20.6 | 21.3 | 22 | 22.8 | 23.5 | 24.3 | 25.1 |
| 36 | (OH-,H-) 4,6-DCDF \rightarrow 4,6-DCDF + H ₂ O | $\Delta_r G^\circ$ | -15.7 | -24 | -27.9 | -31.6 | -35.4 | -42.7 | -46.4 | -49.9 |
| | | ΔG^\ddagger | 45.3 | 45.4 | 45.5 | 45.6 | 45.6 | 45.7 | 45.8 | 45.9 |
| 37 | enol-enol \rightarrow H ₂ O + 4,6-DCDF | $\Delta_r G^\circ$ | 3.8 | 0.1 | -3.5 | -7.0 | -10.5 | -13.9 | -17.3 | -20.6 |
| | | ΔG^\ddagger | 62.4 | 62.2 | 62.0 | 61.7 | 61.4 | 61.0 | 60.7 | 60.3 |

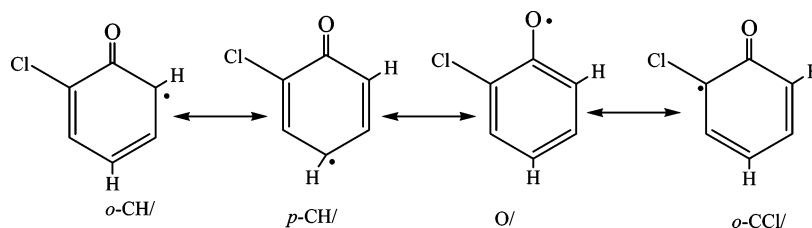
^a In reference to Figure 7.

group of one 2-chlorophenol molecule on the *ortho*-bonded Cl atom on the other 2-chlorophenol to produce the predioxin structure preD1 is energetically preferred over elimination of H₂ from combination of *ortho*-bonded H with the hydroxyl

group hydrogen to produce the predioxin structure preD2. Both processes are found to occur in one step through the transition structures TS1(preD1) and TS(preD2) displayed in Figure 4. As indicated in Table 2, both reactions exhibit substantial

TABLE 5: Values of $\Delta_r G^\circ$ and ΔG^\ddagger (kcal/mol) for Reactions Leading to Formation of 4-MCDF from D2^a

| no. | T (K) | | 298.15 | 400 | 500 | 600 | 700 | 800 | 900 | 1000 |
|-----|---|---------------------|--------|-------|-------|-------|-------|-------|-------|-------|
| 38 | D2 + H \rightarrow HCl + keto-keto \cdot | $\Delta_r G^\circ$ | -75.0 | -76.0 | -77.0 | -78.2 | -79.0 | -80.0 | -81.0 | -82.0 |
| | | ΔG^\ddagger | 8.3 | 10.2 | 12.1 | 14.0 | 15.9 | 17.9 | 19.8 | 21.8 |
| 39 | D2 + OH \rightarrow HOCl + keto-keto \cdot | $\Delta_r G^\circ$ | -24.0 | -25.0 | -26.0 | -26.6 | -27 | -28.2 | -29 | -30 |
| | | ΔG^\ddagger | 5.6 | 8.3 | 11.0 | 13.6 | 16.3 | 18.9 | 21.5 | 24.1 |
| 40 | keto-keto \cdot \rightarrow enol-keto \cdot | $\Delta_r G^\circ$ | -26.3 | -26 | -25 | -24.7 | -24 | -23.5 | -23.0 | -22.0 |
| | | ΔG^\ddagger | 48.6 | 48.9 | 49.2 | 49.5 | 49.9 | 50.2 | 50.6 | 50.9 |
| 41 | enol-keto \cdot \rightarrow (OH-) 4-MCDF | $\Delta_r G^\circ$ | 18.6 | 18.7 | 18.9 | 19.1 | 19.2 | 19.3 | 19.4 | 19.5 |
| | | ΔG^\ddagger | 32.1 | 32.4 | 32.6 | 32.9 | 33.2 | 33.5 | 33.8 | 34.2 |
| 42 | (OH-) 4-MCDF \rightarrow OH + 4-MCDF | $\Delta_r G^\circ$ | 5.2 | 2.0 | -1.1 | -4.3 | -7.3 | -10.4 | -13 | -16.0 |
| | | ΔG^\ddagger | 14.2 | 14.1 | 13.9 | 13.9 | 13.8 | 13.7 | 13.7 | 13.7 |

^a In reference to Figure 9.**Figure 8.** Resonance forms of the 2-chlorophenoxy radical.**TABLE 6: Reaction ($\Delta_r E^\circ$) and Activation (E_a) Energies (at 0 K) Computed at the UB3LYP/6-311+G(3df,2p)//UB3LYP/6-31G(d) Level of Theory for the Coupling Reactions of Two 2-Chlorophenoxy Radicals To Give D1–D9**

| structure | reaction energy (kcal/mol) | activation energy (kcal/mol) | structure | reaction energy (kcal/mol) | activation energy (kcal/mol) |
|-----------|----------------------------|------------------------------|-----------|----------------------------|------------------------------|
| D1 | -8.1 | 9.4 | D6 | -5.7 | no ^a |
| D2 | 2.1 | 15.1 | D7 | -3.5 | 12.7 |
| D3 | 8.8 | 19.1 | D8 | -14.4 | no ^a |
| D4 | -17.0 | 1.2 | D9 | -6.2 | 8.9 |
| D5 | -12.9 | 9.0 | | | |

^a Denotes a barrierless process. No transition structure is found at this level of theory.

temperature-dependent energy barriers. Thus, it is unlikely that 1-MCDD, which is the major product from the pyrolysis of 2-chlorophenol, forms from the direct elimination of H₂ between two 2-chlorophenol molecules but rather through radical + molecule and/or radical + radical pathways.

Figure 5 depicts three pathways for coupling between 2-chlorophenoxy and 2-chlorophenol, including both reaction and activation energies at 0 K. Along the uppermost pathway, the oxygen-centered radical combines with 2-chlorophenol eliminating a Cl radical and producing a predioxin structure of preD1 in a one-step reaction; Figure 4 illustrates the transition state, i.e., TS2(preD1). Note that this radical–molecule pathway has a significantly lower activation barrier (see Table 2) than the molecule–molecule pathways of Figure 3. Following the middle pathway of Figure 5, the hydrogen atom of the hydroxyl group in 2-chlorophenol combines with the chlorine atom of 2-chlorophenoxy producing the predioxin structure 2-(2-chlorophenoxy)cyclohexa-2,5-dienone (preD3). This pathway involves the elimination of HCl through TS(preD3), illustrated in Figure 4, in a one-step reaction similar to the upper reaction of Figure 3. Finally, along the lower pathway of Figure 5, the phenolic oxygen is added to the C6 position in 2-chlorophenol and the predioxin structure, 2-chloro-6-(2-chlorophenoxy)-cyclohexa-1,4-dienol (preD4) forms, with a similar activation energy as that of the uppermost pathway.

All the predioxins (D5, D8, preD1–4) have noncoplanar structures. Dimerization of these compounds into DD and 1-MCDD involves reactions with radicals, intramolecular

hydrogen transfers, and ring closure processes. A schematic description of these processes is presented in Figure 6. The bond between the chlorine and carbon attached to the O bridge in D8 is significantly elongated ($R_{C-Cl} = 1.913$ Å), thus this chlorine atom should be easily abstracted by radicals, especially H, Cl, and OH. Cl abstraction by H from this site under pyrolysis conditions is calculated to have a barrier of only 0.7 kcal/mol at 0 K. However, ΔG^\ddagger attains 4.8, 7.8, and 15.8 kcal/mol at 298.15, 500, and 1000 K, respectively, as indicated in Table 3 in a process characterized by $\Delta_r G^\circ$ of -66.6, -72.4, -75, and -80.0 kcal/mol, at 0, 298.15, 500, and 1000 K, respectively. Abstraction by OH has a trivial barrier of 1.4 kcal/mol at 0 K, but the entropic contribution increases this barrier to 9.0, 14.1, and 26.9 kcal/mol at 298.15, 500, and 1000 K, respectively. Finally, Cl can readily be abstracted from D8 by another Cl forming the direct predioxin precursor, the keto-ether structure of preD3. Intra-annular elimination of Cl from preD3 yields dibenzo-*p*-dioxin (DD), requiring a barrier of 26.5 kcal/mol at 0 K. Although this step displays endoergicity of 22.7 kcal/mol at 0 K, the reaction becomes exoergic at about 800 K, as a consequence of the influence of the entropy change of the reaction.

Another possible pathway for the formation of DD is through preD1 which forms through radical–molecule coupling. A direct route for formation of DD from preD1 involves unimolecular elimination of HCl (see Figure 6). This elimination, however, requires the activation energy of 56.1 kcal/mol at 0 K increasing slightly when compared with its corresponding ΔG^\ddagger values in Table 2. Although the reaction is slightly endoergic at 0 K, $\Delta_r G^\circ$ increases to 13.6, 19.4, and 32.0 kcal/mol, 298.15, 500, and 1000 K, respectively.

The molecule–radical pathway for the formation of DD is not competitive with the radical–radical pathway unless the abstraction of the hydrogen atom of the hydroxyl group in preD1 by H and OH radicals is considered. Abstractions of the hydrogen of the hydroxyl group by H and OH radicals, to yield the keto-ether dioxin precursor preD3, have trivial barriers at 0 K, and, similarly to other reactions involving radicals investigated in this study, with the barriers displaying temperature dependence; see reactions 19 and 20 in Table 3. These reactions are significantly exothermic with 24.5 and 35.3 kcal/mol excess energy for abstraction by H and OH, respectively

at 0 K. $\Delta_r G^\circ$ remains relatively constant for these two reactions, throughout the considered temperature range.

1-Monochlorodibenzo-*p*-dioxin (1-MCDD) is the major pyrolysis¹⁸ product of 2-chlorophenol and is also the major product of oxidation at low inlet concentration of 2-chlorophenol¹⁷ and at relatively low temperature²¹ (375 K). The lower portion of Figure 6 shows the energies of 1-MCDD formation from D5 by radical–radical coupling. H abstraction by H and OH from D5 to produce the chlorinated diphenyl ether, preD5, is highly exothermic with low-energy barriers. Ring closure of preD5 forms 1-MCDD upon intra-annular elimination of Cl with a barrier of 27.3 kcal/mol at 0 K. ΔG^\ddagger values for this reaction are very similar to that for Cl elimination from preD3 to form DD. Alternatively, hydrogen atom transfer to the phenolic oxygen (tautomerization) through preD2 incurs significant barrier as does its second step of HCl unimolecular elimination to form 1-MCDD. The predioxin structure of preD4 which results through radical–molecule coupling (see Figure 5) could also serve as a precursor for 1-MCDD formation upon abstraction of the H atom attached to the carbon at the end of the O bridge, followed by unimolecular elimination of HCl.

Formation of Polychlorinated Dibenzofurans. Formation of polychlorinated dibenzofurans (PCDF) through molecule–molecule or radical–molecule coupling incurs high endothermicity because these reactions involve the displacement of the hydroxyl group of 2-chlorophenol by 2-chlorophenoxy.^{16,17} Thus, the most feasible route to the formation of PCDF in the gas phase is through radical–radical combinations. Previous ab initio studies^{16,23} have focused on the formation of nonchlorinated dibenzofurans (DF) from a keto–keto structure resulting from the coupling of two phenoxy radicals both at the *ortho* positions. The keto–keto^{16,23} structure must transfer to a keto–enol structure (closed shell pathway) or enol–enol structure (open shell pathway) in order to form DF + H₂O. As is documented in the literature, only chlorinated phenoxy radicals which both have *ortho* carbon hydrogen-bearing sites can form chlorinated DF (PCDF).

In experimental gas-phase oxidation studies, the major product^{19–22,34–35} was found to be 4,6-dichlorodibenzofuran (4,6-DCDF). Evans et al.¹⁹ have proposed mechanisms to account for its formation. We have carried out quantum chemical calculations on their mechanisms, and our results are summarized in Figure 7 and Table 4. Two routes to 4,6-DCDF have been proposed: the first is the bimolecular pathway (Scheme 1 in Figure 7) and the second is the unimolecular route (Scheme 2 in Figure 7). Radical–radical coupling of two 2-chlorophenoxy radicals both at the carbon-hydrogen centered radical mesomer would result in the formation of the diketo dimer, D1.

In Scheme 2, hydrogen transfer reactions from the diketo dimer D1 lead to the formation of 4,6-DCDF via different routes. The first step is a single hydrogen atom transfer to the neighboring oxygen keto atom to form 2-chloro-6-(3-chloro-2-hydroxyphenyl)cyclohexa-2,4-dienone (a chlorinated enol–keto structure). This hydrogen transfer process proceeds through a high activation barrier of 53.0 kcal/mol and is exoergic by 18.1 kcal/mol at 0 K. According to our DFT calculations, this enol–keto structure may undergo another hydrogen transfer process (double enolization) to produce the bis-enol dimer of 3,3'-dichlorobiphenyl-2,2-diol (a chlorinated *o,o'*-dihydroxybiphenyl (DHOB)). Transformation of the enol–keto dimer into the enol–enol (bis-enol) structure could proceed via two different transition structures (see Figure 7). The first involves a concerted concentric movement of two hydrogen atoms between the keto-oxygen and the enol-oxygen atoms and between the carbon and

the keto-oxygen atoms. This transition structure has an energy barrier which is 23.4 kcal/mol at 0 K less than the second transition structure which resembles the hydrogen movement between the keto-oxygen and the carbon atom. The enol–enol dimer is located 26.7 kcal/mol below the enol–keto dimer. Alternatively, the enol–keto dimer may transfer directly to a (H-,OH-) 4,6-DCDF intermediate, through an energy barrier of 29.3 kcal at 0 K. Thus, the transformation of the keto–enol into this intermediate is less favorable than its transformation to the enol–enol structure through the first transition structure.

In our DFT calculations, we were unable to locate a direct route from D1 to either the enol–enol or the (H-,OH-) 4,6-DCDF intermediates. Formation of the keto–enol structure via the large activation barrier (53.0 kcal/mol) is a prerequisite for the formation of the enol–enol structure and the (H-,OH-) 4,6-DCDF intermediate. In a previous ab initio study, a direct route was found for nonchlorinated phenoxy radicals.²³ Additionally, in that study²³ only a second-order saddle point could be found for the concerted double hydrogen atom migration to the keto oxygen atoms. That study²³ also found an energy barrier of 15 kcal/mol for the formation of (H-,OH-) DF from the (R,S) keto–keto mesomer of *o,o'*-dihydroxybiphenyl (DHOB) dimer. Detailed IRC calculations for these two stationary states would be required to verify the exact path that these two states actually connect.

Dehydration reactions for both the (H-, OH-) 4,6-DCDF intermediate and the enol–enol intermediate can lead to the formation of 4,6-DCDF (see Figure 7). Both routes have large barriers; expulsion of H₂O from the enol–enol structure together with ring closure to form 4,6-DCDF has a barrier 23.8 kcal/mol higher than the route from the (H-, OH-) 4,6-DCDF intermediate.

In the combustion environment, active radicals, especially OH and H, will greatly facilitate the formation of PCDD/PCDF. In Scheme 1 of Figure 7, we carried out a DFT study of an alternative pathway for the formation of 4,6-DCDF. This pathway is initiated by H abstraction from the C–C bridge of D1 by H and OH radicals. Both abstractions have trivial energy barriers and are highly exoergic. The remaining H atom in the resulting keto–keto' structure can then undergo tautomerization where an H atom migrates to the keto O atom. This process has a significant barrier of 48.1 kcal/mol and results in an enol–keto' intermediate. Ring closure of this enol–keto' intermediate involves a barrier of 30.3 kcal/mol and is endoergic by 18 kcal/mol. It results in the formation of a precursor of 4,6-DCDF with an out-of-plane OH moiety attached at C5. The carbon–oxygen bond here is significantly elongated ($R_{C-OH} = 1.414$ Å). Hence, a transition structure with a relatively small energy barrier of 14.8 kcal/mol has been found for the expulsion of OH and the formation of 4,6-DCDF. Thus, according to our DFT calculations, the preferred route to PCDF formation would appear to proceed through the formation of enol–keto' intermediates. However, we can calculate from Table 6 that the activation energy for the reverse dissociation reaction for D1 is 17.8 kcal/mol. This is significantly less than the activation energy for the formation of the keto–enol intermediate (53.0 kcal/mol). These conclusions are in contrast with a previous study¹⁶ using HF/3-21G and AM1 methods, which found that the reverse dissociation activation energy is comparable with the activation energy for the formation of the partially enolized structure, keto–enol, at least, for the nonchlorinated system. For the nonchlorinated system, the keto–enol structure could only be located¹⁶ at the HF/3-21G(d) level of theory but could not be found²³ at the B3LYP/6-31G(d) level of theory. Our

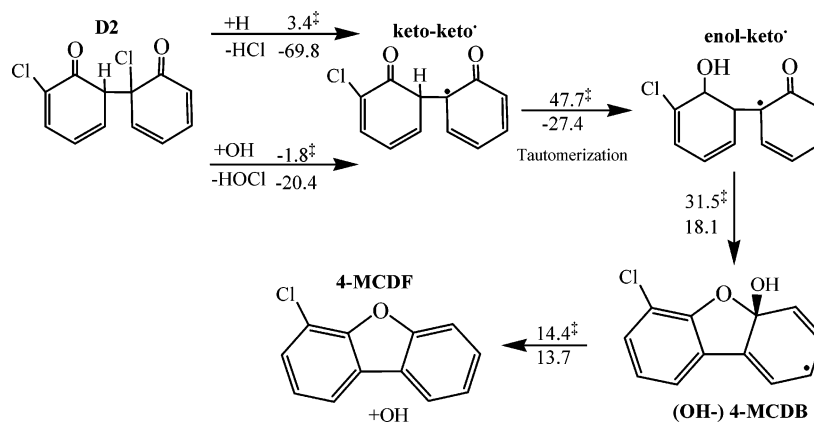


Figure 9. Formation of 4-MCDF from 1,3'-dichloro-1,1'-bi(cyclohexa-3,5-diene)-2,2-dione (D2). Symbol ‡ denotes activation energies, and the other values are the reaction energies at 0 K, both calculated at the B3LYP/6-311+G(3df,2p)//B3LYP/6-31G(d) level of theory.

results lead to the conclusion that the unimolecular route (Scheme 2) to 4,6-DCDF is not competitive with the bimolecular route (Scheme 1), and it is by the latter route that the product is produced in oxidation of 2-chlorophenol.

Consider now the explanation of the experimental observation that 1-MCDD is produced in higher yield than 4,6-DCDF in oxidation^{17,21} and pyrolysis¹⁸ of 2-chlorophenol. Although combination of two 2-chlorophenoxy radicals, as indicated by the data of Tables 1 and 6, will not produce significantly different concentrations of the respective precursors D5 and D1, the barrier for subsequent conversion of D5 into 1-MCDD (Figure 6) is significantly lower (27.3 versus 48.1 kcal/mol) than the minimum barrier for formation of 4,6-DCDF from D1 (Figure 7, Scheme 1).

Figure 9 and Table 5 summarize the thermochemical parameters for the formation of 4-MCDF. This isomer has been observed in oxidation but not in pyrolysis of 2-chlorophenol. Our DFT calculations show that the bridge Cl in D2 can readily be abstracted by either H or OH in combustion. However, as shown in Figure 9, there is a significant tautomerization barrier preceding formation of 4-MCDF. The abstraction of Cl from D2 by H and OH exhibits strong entropic effects, which are evident by comparing ΔG^\ddagger at 0 K (i.e., E_a) in Figure 9, with ΔG^\ddagger in Table 5 (reactions 38 and 39). The Gibbs free energy change of the hydroxyl elimination reaction (reaction 42 in Table 6) displays evident temperature sensitivity, further highlighting the influence of entropy on the formation pathway of 4-MCDF. Note that similar observations can be made for reactions 28 and 29 (for ΔG^\ddagger) and reactions 32 and 36 (for $\Delta_r G^\circ$) in Table 4, demonstrating the effect of entropy on the formation of 4,6-DCDF, as well.

Conclusions

Reaction and activation energies defining the mechanisms of formation of PCDD/PCDF from oxidation and pyrolysis of 2-chlorophenols have been calculated using DFT theory. Two channels for molecule–molecule interactions, three channels for molecule–radical interactions, and nine channels for radical–radical interactions have been investigated for the formation of DD, 1-MCDD, 4,6-DCDF, and 4-MCDF, the main dioxin products observed experimentally in combustion and/or pyrolysis of 2-chlorophenol. Different coupling modes of 2-chlorophenoxy define the formation of different dioxin products. In total, Gibbs free-energy data have been generated for 42 key reactions in the gas-phase formation of PCDD/PCDF from 2-chlorophenol, for temperature up to 1000 K.

Large entropic penalties incurred with increasing temperatures for the 15 coupling modes of chlorophenols and chlorophenoxy

(Tables 1 and 2) could make the self-condensation of chlorophenols and chlorophenoxy less favorable at higher temperatures. Active radicals such as H and OH have been shown to provide pathways of lowest barriers in formation of both PCDD/PCDF when compared with competing unimolecular routes.

Formation of the predioxin structures of preD3 and preD5 from 2-chlorophenoxy coupling products of D5 and D8, through the radical derived pathways, constitute the major corridor for the most abundant dioxin products both under oxidative and pyrolytic conditions, as a consequence of the low-energy barriers and exergonicity. The reaction steps requiring the largest barriers in PCDD formation are intra-annular eliminations of Cl and HCl (Figure 6).

Keto–keto $^\bullet$ species form through exergonic reactions of H and OH radicals with D1 and D2. Thus, these keto–keto $^\bullet$ species initiate the most accessible pathways for the formation of PCDF; i.e., 4,6-DCDF and 4-MCDF. The reaction steps necessitating the largest barriers in the production of PCDF involve single or double enolization of the bis-keto dimer (Scheme 2 in Figure 7).

Acknowledgment. This research has been supported by a grant from the Australian Research Council. M.A. acknowledges the award of a postgraduate studentship by the Al-Hussein Bin Talal University (Jordan). The authors acknowledge the access to the computational facilities of the Australian Centre of Advanced Computing and Communications (ac3). We also thank a reviewer for helpful comments on locating transition structures on open-shell hypersurfaces.

Supporting Information Available: Calculated total energies, zero point energies, Cartesian coordinates, rotational constants, and vibrational frequencies of all equilibrium and transition structures. This material is available free of charge via the Internet at <http://pubs.acs.org>.

References and Notes

- Altwicker, E. R. *Chemosphere* **1996**, *33*, 1897.
- Altwicker, E. R.; Milligan, M. S. *Chemosphere* **1993**, *27*, 301.
- Karasek, F. W.; Dickson, L. C. *Science* **1987**, *237*, 754.
- Milligan, M. S.; Altwicker, E. R. *Environ. Sci. Technol.* **1996**, *30*, 225.
- Khachatryan, L.; Asatryan, R.; Dellinger, B. *Chemosphere* **2003**, *52*, 695.
- Khachatryan, L.; Burcat, A.; Dellinger, B. *Combust. Flame* **2003**, *132*, 406.
- Hung, H.; Buekens, A. *Chemosphere* **1999**, *38*, 1595.
- Sidhu, S. S.; Maqsood, L.; Dellinger, B.; Mascolo, G. *Combust. Flame* **1995**, *100*, 11.

- (9) Babushok, V.; Tsang, W. *7th International Congress on Combustion By-Products: Origins, Fate, and Health Effects*; Research Triangle Park, North Carolina, 2001; p 36.
- (10) Berho, F.; Lesclaux, R. *Chem. Phys. Lett.* **1997**, *279*, 289.
- (11) Wiater-Protas, I.; Louw, R. *Eur. J. Org. Chem.* **2001**, *20*, 3945.
- (12) Shaub, W. M.; Tsang, W. *Environ. Sci. Technol.* **1983**, *17*, 721.
- (13) Bruce, K.; Beach, L. O.; Gullett, B. K. *Waste Manage.* **1983**, *11*, 97.
- (14) Altwicker, E. R. *Sci. Total Environ.* **1991**, *104*, 47.
- (15) Wiater, I.; Born, J. G. P.; Louw, R. *Eur. J. Org. Chem.* **2000**, *6*, 921.
- (16) Khachatryan, L.; Asatryan, R.; Dellinger, B. *J. Phys. Chem. A* **2004**, *108*, 9567.
- (17) Sidhu, S.; Edwards, P. *Int. J. Chem. Kinet.* **2002**, *34*, 531.
- (18) Evans, C. S.; Dellinger, B. *Environ. Sci. Technol.* **2003**, *37*, 1325.
- (19) Evans, C. S.; Dellinger, B. *Environ. Sci. Technol.* **2005**, *39*, 122–127.
- (20) Mulholland, J. A.; Akki, U.; Yang, Y.; Ryu, J. Y. *Chemosphere* **2001**, *42*, 719.
- (21) Weber, R.; Hagenmaier, H. *Chemosphere* **1999**, *38*, 529.
- (22) Louw, R.; Ahonkhai, S. T. *Chemosphere* **2002**, *46*, 1273.
- (23) Asatryan, R.; Khachatryan, L.; Dellinger, B. *J. Phys. Chem. A* **2005**, *109*, 11198.
- (24) Janoschek, R.; Fabian, W. M. F. *J. Mol. Struct.* **2003**, *635*, 661–662.
- (25) Zhu L.; Bozzelli J. W. *J. Phys. Chem. A* **2003**, *107*, 3696.
- (26) Asatryan, R.; Davtyan, A.; Catherine, S. E.; Dellinger, B. *Organohalogen Compd.* **2002**, *56*, 277.
- (27) Okamoto, Y.; Tomonari, M. *J. Phys. Chem. A* **1999**, *103*, 7686.
- (28) Frisch, M. J.; Trucks, G. W.; Schlegel, H. B.; Scuseria, G. E.; Robb, M. A.; Cheeseman, J. R.; Zakrzewski, V. G.; Montgomery, J. A.; Stratmann, R. E.; Burant, J. C.; Dapprich, S.; Millam, J. M.; Daniels, R. E.; Kudin, K. N.; Strain, M. C.; Farkas, O.; Tomasi, J.; Barone, V.; Cossi, M.; Cammi, R.; Mennucci, B.; Pomelli, C.; Adamo, C.; Clifford, S.; Ochterski, J.; Petersson, G. A.; Ayala, P. Y.; Cui, Q.; Morokuma, K.; Salvador, P.; Dannenberg, J. J.; Malick, D. K.; Rabuck, A. D.; Raghavachari, K.; Foresman, J. B.; Cioslowski, J.; Ortiz, J. V.; Baboul, A. G.; Stefanov, B. B.; Liu, G.; Liashenko, A.; Piskorz, P.; Komaromi, I.; Gomperts, R.; Martin, R. L.; Fox, D. J.; Keith, T.; Al-Laham, M. A.; Peng, C. Y.; Nanayakkara, A.; Challacombe, M.; Gill, P. M. W.; Johnson, B.; Chen, W.; Wong, M. W.; Andres, J. L.; Gonzalez, C. M.; Head-Gordon, M.; Replogle, E. S.; Pople, J. A. *Gaussian 03, revision A.11*; Gaussian, Inc.: Pittsburgh, PA, 2001.
- (29) Becke, A. D. *J. Chem. Phys.* **1993**, *98*, 5648.
- (30) Lee, C.; Yang, W.; Parr, R. G. *Phys. Rev. B* **1988**, *37*, 785.
- (31) Montgomery, J. A.; Ochterski, J. W.; Petersson, G. J. *Chem. Phys.* **1994**, *101*, 5900.
- (32) Zhu, L.; Bozzelli, J. W. *J. Phys. Chem. Ref. Data* **2003**, *32*, 1713.
- (33) Bozzelli, J. W.; Desai, V.; Ritter, E. R.; Dean, A. M. *ACS Div. Fuel Chem.* **1991**, *36* (4), 1494.
- (34) Sawersyn, J. P.; Briois, C.; Visez, N.; Baillet, C. *Organohalogen Compd.* **2002**, *66*, 1078.
- (35) Akki, U.; Mulholland, J. A. *Organohalogen Compd.* **1997**, *31*, 475.
- (36) Kim, D.; Mulholland, J. A. *Environ. Sci. Technol.* **2005**, *39*, 5836.